analytical chemistry

Article

pubs.acs.org/ac

XPS Analysis of Enzyme and Mediator at the Surface of a Layer-by-Layer Self-Assembled Wired Enzyme Electrode

Pablo Scodeller,[†] Federico J. Williams, and Ernesto J. Calvo*

INQUIMAE, Facultad de Ciencias Exactas y Naturales, Universidad de Buenos Aires, Pabellon 2, Ciudad Universitaria, AR-1428, Buenos Aires, Argentina

ABSTRACT: High potential purified *Trametes trogii* laccase has been deposited in mono- and multilayer thin films on gold surfaces by layer-by-layer electrostatic adsorption self-assembly. The osmium bipyridil redox relay sites on polycation poly(allylamine) backbone efficiently work as a molecular "wire" in oxygen cathodes for biofuel cells. X-ray photoelectron spectroscopy of Cu 2p3/2 and Os 4f signals provided chemical information on the enzyme and redox mediator surface concentrations after different adsorption steps. The electrical charge involved in oxidation−reduction cycles of the osmium sites, the ellipsometric enzyme film thickness, and the mass uptake from quartz crystal microbalance experiments, correlate with the XPS surface concentration, which provides unique evidence on the chemical identity of the composition in the topmost layers. XPS is shown to be an important analytical tool to investigate stratified copper and osmium distribution in LbL thin films relevant to biosensors and biofuel cells.

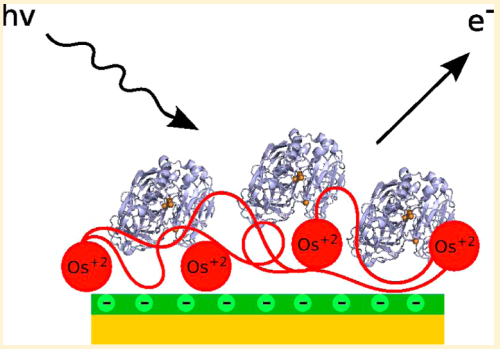

The multicopper enzyme laccase (EC1.10.3.2; benzenediol: oxygen oxido-reductase) is an extracellular blue copper enzyme in plants and fungi which catalyzes the oxidation of biphenols and the four-electron reduction of molecular oxygen to water at high potentials.[1−3] The enzyme contains four copper atoms, denoted T1, T2, and T3 according to their spectroscopic properties. In high potential laccases, the copper center T1 can be reduced by phenol compounds, one-electron redox mediators and direct electron transfer from electrodes. While substrates are oxidized at T1 copper site, further internal electron transfer leads to the reduction of molecular O_2 at the trinuclear T2/T3 cluster.[4−7] Direct electron transfer from metal or carbon electrodes to laccase has been reported,[8−12] and this depends critically on the surface protein orientation,[13,14] as well as on carbon electrode surfaces modified with linkers.[15−18]

In previous communications, we have reported the electrocatalysis toward oxygen reduction by self-assembled layer-by-layer (LbL) multilayers of *Trametes trogii* laccase by sequential electrostatic adsorption of an osmium bipyridil modified poly(allylamine) polyelectrolyte (PAH-Os) and laccase (Lac) on mercapto-propanesulfonate (MPS) modified gold surfaces.[19,20]

Gero Decher[21] introduced, in 1991, the layer by layer (LbL) technique to form organized multilayer films on solid substrates by alternate adsorption of anionic and cationic polyelectrolytes. The strategy was extended to the adsorption of proteins and to the development of amperometric enzyme electrodes based on layer-by-layer (LbL) self-assembled enzyme and redox mediator multilayers pioneered by Hodak et al. in 1997.[22] Since then an extensive literature has been published by our research group and others on amperometric enzyme electrodes comprised of LbL organized enzyme multilayers.[23] In these organized LbL structures, a much better control over the position of the redox polyelectrolyte with respect to the enzyme molecules than in random hydrogels built with the same components can be achieved, and spatially organized multilayers with mono and bienzymatic schemes can work efficiently in molecular recognition, redox mediation, and generation of an electrical signal in biosensors.[24]

Successive redox polymer mediator (osmium complex tethered to polyallylamine backbone) and laccase (Lac) layers can be deposited by alternate immersion of the thiol-modified Au in the respective polyelectrolyte and enzyme solutions at suitable pH where the enzymes and polyelectrolytes exhibit the excess charge needed in the electrostatic self-assembly process.[25]

In layer by layer deposition, it is expected that the enzyme film thickness, the surface concentration of redox sites and the enzyme loading grow with the number of adsorption steps. The enzyme catalyzed current toward the substrate oxygen increases with the film thickness following the redox charge propagation within the film by a sequence of electron hopping events between some suitably positioned laccase T1 Cu redox centers.

In their early work, Laurent and Schlenoff[26] showed that there is interpenetration between layers of poly(styrenesulfonate) and poly(butanylviologen) using variable-angle XPS, which revealed a 1:1 stoichiometry between charges on positive and negative polyelectrolytes. Rusling and co-workers also employed XPS to detect the nitrogen peak (N 1s)

Received: August 21, 2014
Accepted: November 24, 2014
Published: November 24, 2014

at 401.5 eV and Si 2p peak SiO_2 in LbL films of SiO_2 nanoparticles and hemoglobin.[27]

Caruso et al.[28] estimated the thickness (d) of poly(allylamines hydrochloride) (PAH) and poly(styrenesulfonate) (PSS) LbL polyelectrolyte films in the dry state adsorbed onto metal substrates from XPS by comparing the intensities for bare Au and the multilayer covered Au using a mean free path of gold photoelectrons in the organic medium of 3.5 nm. The internal layered structure of LbL polyelectrolyte multilayers was demonstrated by the group of Decher with Neutron and X-ray Reflectivity measurements.[21]

In the work reported here, we show for the first time X-ray photoelectron spectroscopy (XPS) analysis of the LbL laccase/osmium polymer stratified multilayers by examination of the Cu 2p3/2 and Os 4f XPS signals for different number of Lac and PAH-Os layers as compared to experimental evidence with quartz crystal microbalance (QCM) mass, ellipsometry thickness and voltammetric osmium redox charge.

EXPERIMENTAL METHODS

3-Mercaptopropyl sulfonate (MPS), potassium nitrate, Na_2HPO_4, and NaH_2PO_4 were purchased from Sigma. Poly(Allylamine) (PAH), sodium acetate, and acetic acid (100%) were from Fluka. All reagents were analytical grade and used without further purification except PAH which was dialyzed against Milli-Q water. Ultrapure water was obtained from a Milli-Q purification system (nominal resistivity 18.2 MΩ at 25 °C) and used to prepare all solutions. The complex $[Os(bpy)_2Cl(PyCOH)]Cl$ (where PyCOH is pyridine carbaldehyde, in this article called "Os complex") and osmium poly(allylamine) (PAH-Os) were synthesized as described elsewhere.[29] Laccase from *Trametes trogii* was purified from stock cultures as described elsewhere.[20] Gold coated Si(100) substrates were employed as surfaces for XPS with 20 nm Ti and a 20 nm Pd adhesion layer and a 200 nm gold layer thermally evaporated using an Edwards Auto 306 vacuum coating system, at $P < 1 \times 10^{-5}$ mbar. The gold surfaces were cleaned by cyclic voltammetry in 2 M sulfuric acid between 0 and 1.6 at 1 V s^{-1}.

Then, in a first step, a monolayer of MPS was formed by immersing the electrodes in a solution of 0.02 M MPS in 0.01 M H_2SO_4 for 30 min. After rinsing the electrodes with Milli-Q water, 100 μL of a solution of 0.44 mM PAH-Os of pH 8 was deposited on the electrode surface and allowed to assemble for 10 min. After it was rinsed, 100 μL of 0.5 mg·mL^{-1} Lac in water was dropped on the same electrode, and after 10 min of self-assembly, the laccase solution was removed, and the modified gold disk was rinsed with Milli-Q water. These deposition steps were repeated until the desired number of polymer and enzyme layers were deposited.

Cyclic voltammetry was performed using an Autolab PGSTAT 30 potentiostat in a three-electrode cell with a platinum gauze as counter electrode and Ag/AgCl/(Cl 3M) as reference electrode (all potentials herein are referred to this reference electrode). For the electrochemical measurements, the working electrodes were gold discs (d = 5 mm) embedded in KelF polymer. All electrochemical measurements were performed in 0.1 M acetate buffer of pH 4.7 containing 0.2 M KNO_3. Before measurements all solutions were degassed with pure argon. Cyclic voltammetry of these electrodes in O_2-free solutions shows only the Os(III)/Os(II) redox couple at 0.31 V allowing us to integrate the total electrical charge at low sweep rate (5 mV·s^{-1}).

The adsorption process was followed by in situ quartz crystal microbalance (QCM) and ellipsometry. A variable angle rotating-analyzer automatic ellipsometer (SE 400 model Sentech GmbH, Germany) equipped with a 632 nm laser as polarized light source was employed to measure the film thicknesses of the electrodes. The quartz crystal resonator at 10 MHz was used as a quartz crystal microbalance (QCM) with a complex voltage divider to measure the resonant frequency and both components of the quartz crystal Butterworth−Van Dyke (BVD) equivalent circuit, which has been described elsewhere. The crystals were mounted in the cells by means of Viton O-ring seals, with only one face in contact with the electrolyte.

X-ray Photoelectron Spectroscopy Measurements (XPS). X-ray photoelectron spectroscopy measurements (XPS) were performed under UHV conditions (base pressure < 5.10^{-10} mbar) in a SPECS UHV spectrometer system equipped with a 150 mm mean radius hemispherical electron energy analyzer and a nine channeltron detector. XPS spectra were acquired at a constant pass energy of 20 eV using an unmonochromated MgKα (1253.6 eV) source operated at 12.5 kV and 20 mA and a detection angle of 30 degrees with respect to the sample normal. Quoted binding energies are referred to the Au 4f7/2 emission at 84 eV. No charge compensation was necessary and no differential charging features were observed (e.g., low BE tails) given that we have measured sufficiently thin films on grounded conducting substrates. Atomic ratios and surface concentrations were calculated from the integrated intensities of core levels after instrumental and photoionization cross-section corrections.

RESULTS AND DISCUSSION

In previous communications, we have described the coimmobilization of *Trametes trogii* laccase and the osmium modified poly(allylamines), PAH-OS, redox mediator by layer-by-layer electrostatic self-assembly to produce oxygen biocathodes.[19,20] Furthermore, in a recent report,[25] we have anticipated that during the adsorption of the enzyme there is no loss of the underlying poly(allylamines), but partial loss of laccase occurs during the adsorption of the redox polyelectrolyte.

In EQCM experiments, the time course of the adsorption steps during the layer-by-layer self-assembly of laccase and PAH-Os can be seen in Figure 1 for the first 6 laccase-osmium polyelectrolyte bilayers. By recording the variation of mass per unit area after the injection of laccase (1), rinse in water (2), and injection of PAH-Os solution in the liquid in contact with the Au coated quartz resonator (3), we can see the uptake and release of material on the surface. In the following, we shall follow the notation of Rubner[30] with integer number of bilayers terminated in laccase and fractional number for PAH-Os capped layers.

The uptake of enzyme is clearly seen by the increase in mass in each enzyme adsorption step followed by a small mass loss during rinsing with water. However, notice that during the adsorption of PAH-Os on the enzyme capped layer an important mass loss is detected which has not been seen in similar LbL experiments with the highly charged enzyme glucose oxidase.[25] In the case of laccase and PAH-Os polyelectrolyte, it is concluded that the local charge in the cationic polyelectrolyte and the low charge density in the enzyme laccase at pH 6 is the cause of the desorption of an important mass of the preadsorbed laccase. The difference in mass before adsorption and after each rinsing step is taken in the deposition cycles as the mass of laccase deposited on the

dx.doi.org/10.1021/ac503147c | Anal. Chem. 2014, 86, 12180−12184

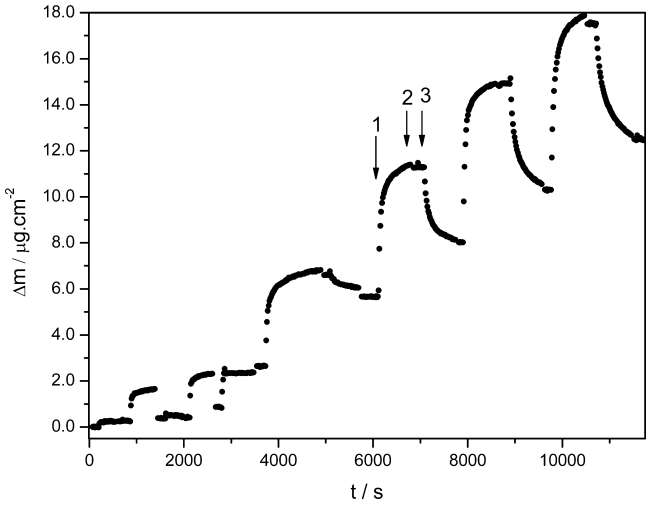

Figure 1. QCM mass uptake during the sequential adsorption of Lac and PAH-Os. Refer to the text for numbers 1, 2, 3.

surface. The average surface concentration of laccase per bilayer, ~4.3 × 10^{-11} mol·cm^{-2}, has been obtained from the laccase mass gain of 2.4 μg·cm^{-2} with a molar mass of 56 kDa determined by Maldi.[20] Notice that this a is a formal mass density since the enzyme is bound to the polycation and does not form a close packed layer.

Upon reaching steady state, the mass uptake and the ellipsometric thickness show a similar zigzag pattern with a decrease in mass and thickness after the adsorption of the osmium derivatized poly(allylamine) as depicted in Figure 2, but a steady increase in thickness and mass in successive complete bilayer adsorptions.

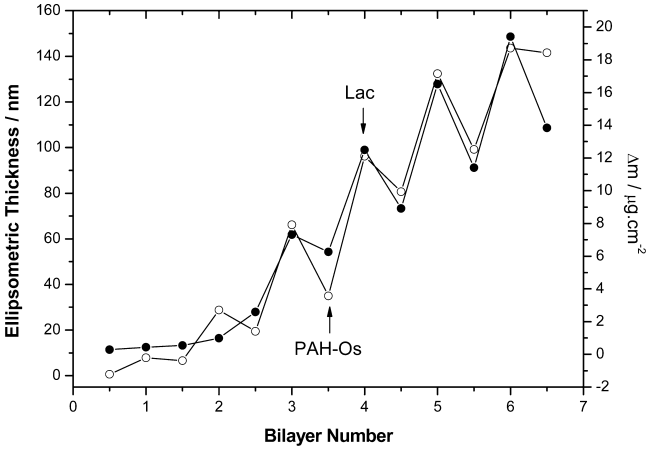

Figure 2. Ellipsometric thickness (open circles) and EQCM mass variation per unit area (solid circles), as a function of number of bilayers for different PAHOs/Lac multilayers. The arrows indicate the macromolecule in the last layer.

The integrated redox charge under slow cyclic voltammetric peaks in the absence of oxygen, on the other hand, exhibits an increase after each adsorption step, even when laccase is desorbed from the surface indicating that there is no loss of redox polymer as shown in Figure 3.

The XPS spectra of $(PAH\text{-}Os/Laccase)_n$ self-assembled multilayers as a function of the number of bilayers n are depicted in Figure 4. Note that integer n implies laccase-

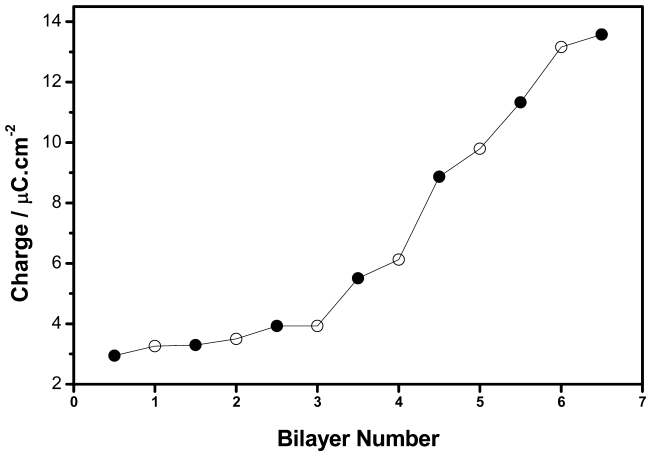

Figure 3. Redox charge as a function of layer number: acetate buffer pH 4.7, 0.1 M + 0.2 M KNO_3; sweep rate 5 mVs^{-1}. Solid circles indicate PAHO-capped electrodes, and open circles indicate laccase-capped electrodes.

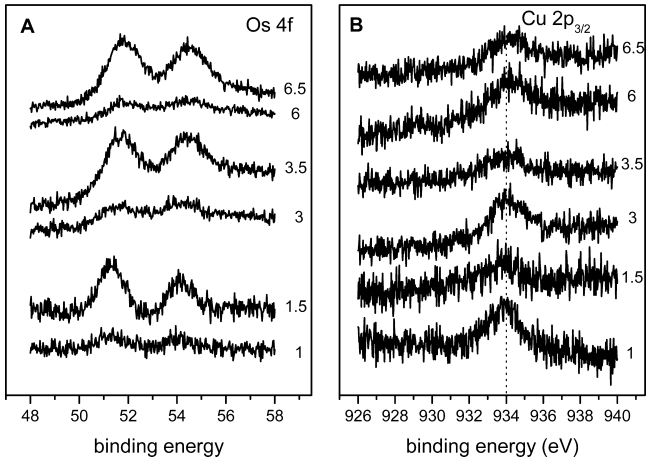

Figure 4. Os 4f (A) and Cu 2p3/2 (B) XPS spectra of $(PAH\text{-}Os/laccase)_n$ self-assembled multilayers. Integer n represent laccase-terminated layers whereas fractional n represents Os-terminated layers.

terminated multilayers, whereas fractional n implies PAH-Os terminated multilayers. Three different LbL laccase-PAH-Os film samples have been measured and the dispersion of data values for osmium and copper is between 5 and 10%, while the detection limit is clearly above the signal-to noise ratio in the spectra shown in Figure 4.

Figure 4A shows the Os 4f XPS spectra as a function of the number of bilayers, n. We observe a doublet corresponding to the 4f7/2 (51.7 eV) and 4f5/2 (54.4 eV) peaks indicating that Os is present in the formal oxidation state +2[31] in all cases. Furthermore, the intensity of the Os 4f XP signal is a strong function of the number of layers and the capping molecules in the layer: PAH-Os-terminated layers exhibit a maximum intensity whereas Laccase terminated layers display smaller intensities. Here we should bear in mind that XPS technique probes the top atomic/molecular layers of the sample (~10 nm depending on the electron attenuation length) and since the present LbL layers are thicker than this value, laccase-terminated layers display a decreased Os signal as the Laccase layer attenuates the Os 4f signal arising from the underlying PAH-Os layers. On the other hand, Figure 4B shows Cu 2p3/2 XPS signal as a function of the number of bilayers, n. We

dx.doi.org/10.1021/ac503147c | Anal. Chem. 2014, 86, 12180−12184

observe a peak with a binding energy of 934 eV that can be assigned to Cu in a formal oxidation state of +2[32] in all cases. The Cu 2p3/2 intensity is a strong function of the topmost layer nature: laccase-terminated layers exhibit the maximum intensity whereas Os-terminated layers show decreased values as shown in Figure 2.

Figure 5 shows Cu 2p3/2 and Os 4f XP integrated intensities as a function of bilayer number *n*. As discussed above laccase-terminated layers (n = 1, 3, and 6) show a maximum Cu intensity and a minimum Os intensity, whereas PAH-Os-terminated layers (n = 1.5, 3.5, 6.5) show the opposite behavior (maximum Os and minimum Cu) as the top layers attenuate the XP signals of the underlying layers. We can make a rough surface coverage estimation from the integrated intensities assuming that the observed signals arise only from the nonattenuated top polyelectrolyte layer. When the Cu signal is maximum the Cu surface concentration is 3.45×10^{13} atoms·cm^{-2} (5.7×10^{-11} mol·cm^{-2}), whereas when the Os signal is maximum the Os surface concentration is 7.6×10^{13} atoms·cm^{-2} (1.3×10^{-10} mol·cm^{-2}).

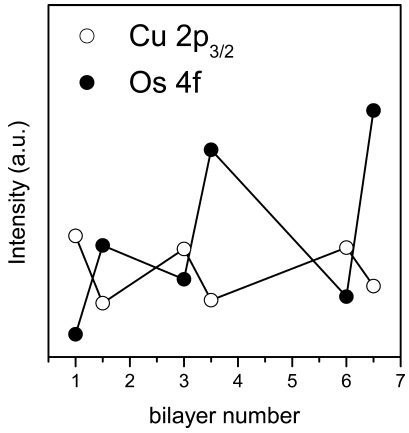

Figure 5. Cu 2p3/2 and Os 4f XP integrated intensities as a function of bilayer number *n*.

The thickness (d) of the self-assembled layer-by-layer film can be estimated from the Au 4f intensity attenuation from $I = I_0 \exp(-d/\lambda \cos\theta)$, where I is the substrate intensity of the film covered surface and I_0 that of the bare substrate, θ is the angle of detection with respect to the surface normal and λ the photoelectron attenuation length. The value of λ for layer-by-layer self-assembled polyelectrolyte films containing proteins is not known, however, as a rough approximation we can use the value of λ corresponding to LbL polyelectrolyte multilayers[28] (3.5 nm) to estimate the film thickness from the decrease in the Au 4f signal. Figure 6 shows the XPS estimated thickness in comparison with the ellipsometric thickness. Clearly as the number of layers deposited increases, both the ellipsometric and XPS film thickness increase as expected. However, the XPS measurement yields a smaller thickness and the difference with the ellipsometric thickness increases with the number of deposited bilayers. We should bear in mind that XPS measurements are carried out in UHV conditions where the films lose water while the ellipsometric measurements correspond to hydrated film. Note however that stratified structure of the multilayer is maintained.

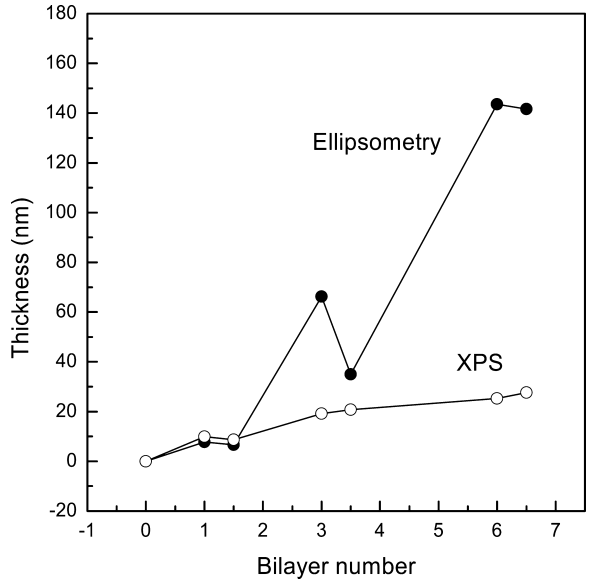

Figure 6. XPS and ellipsometric thickness estimations as a function of bilayer number *n*.

CONCLUSIONS

Both osmium and copper atoms in the topmost layer of LbL multilayers comprised of the blue copper enzyme laccase and the redox polyelectrolyte, PAH-Os could be detected by the respective XPS signals at very low surface concentration, that is, 10^{-11} mol·cm^{-2} copper atoms and 10^{-10} mol·cm^{-2} osmium atoms on the surface. The surface concentrations determined by XPS are in very good agreement with EQCM mass per unit area and the integrated charge of the osmium complex. To the best knowledge of the authors, this is the first use of XPS to measure the surface concentration of a copper enzyme.

The stratified structure of LbL dry multilayer films of laccase and PAH-Os is preserved in the UHV as shown by the photoelectron intensity attenuation due to the organic multilayer. The XPS dry film thickness increases with the number of layers and correlates with the ellipsometric thickness and areal mass increase in successive layers.

The analytical evidence disclosed in the present paper is relevant to the design of enzyme multilayer electrodes with application to biosensor and biofuel cells. While EQCM, ellipsometry can detect very small changes in mass and thickness, XPS provides unique evidence of the chemical identiy of the surface topmost layer with great sensitivity and nanometer height resolution.

AUTHOR INFORMATION

Corresponding Author

*E-mail: calvo@qi.fcen.uba.ar.

Present Address

[†]P.S.: Sanford-Burnham Medical Research Institute, 10901 North Torrey Pines Rd, La Jolla, CA 92037.

Author Contributions

All authors contributed equally.

Notes

The authors declare no competing financial interest.

■ ACKNOWLEDGMENTS

Financial support from CONICET, University of Buenos Aires, and ANPCyT grant PICT 2008 No. 2037 are greatly acknowledged.

■ REFERENCES

(1) Solomon, E. I.; Baldwin, M. J.; Lowery, M. D. *Chem. Rev.* **1992**, *92*, 521−542.
(2) Solomon, E. I.; Augustine, A. J.; Yoon, J. *Dalton Trans.* **2008**, 3921−3932.
(3) Solomon, E. I.; Sundaram, U. M.; Machonkin, T. E. *Chem. Rev.* **1996**, *96*, 2563−2605.
(4) Tarasevich, M. R.; Bogdanovskaya, V. A.; Kuznetsova, L. N. *Russ. J. Electrochem.* **2001**, *37*, 833−837.
(5) Palmore, G. T. R.; Kim, H. H. *J. Electroanal. Chem.* **1999**, *464*, 110−117.
(6) Chen, T.; Barton, S. C.; Binyamin, G.; Gao, Z. Q.; Zhang, Y. C.; Kim, H. H.; Heller, A. *J. Am. Chem. Soc.* **2001**, *123*, 8630−8631.
(7) Calabrese Barton, S.; Kim, H. H.; Binyamin, G.; Zhang, Y.; Heller, A. *J. Am. Chem. Soc.* **2001**, *123*, 5802−5803.
(8) Salaj-Kosla, U.; Poeller, S.; Schuhmann, W.; Shleev, S.; Magner, E. *Bioelectrochemistry* **2013**, *91*, 15−20.
(9) Shleev, S.; Jarosz-Wilkolazka, A.; Khalunina, A.; Morozova, O.; Yaropolov, A.; Ruzgas, T.; Gorton, L. *Bioelectrochemistry* **2005**, *67*, 115−124.
(10) Shleev, S.; Pita, M.; Yaropolov, A. I.; Ruzgas, T.; Gorton, L. *Electroanalysis* **2006**, *18*, 1901−1908.
(11) Shleev, S.; Tkac, J.; Christenson, A.; Ruzgas, T.; Yaropolov, A. I.; Whittaker, J. W.; Gorton, L. *Biosens. Bioelectron.* **2005**, *20*, 2517−2554.
(12) Salaj-Kosla, U.; Poeller, S.; Schuhmann, W.; Shleev, S.; Magner, E. *Bioelectrochemistry* **2013**, *91*, 15−20.
(13) Climent, V.; Zhang, J.; Friis, E. P.; Østergaard, L. H.; Ulstrup, J. *J. Phys. Chem. C* **2012**, *116*, 1232−1243.
(14) Pita, M.; Gutierrez-Sanchez, C.; Olea, D.; Velez, M.; Garcia-Diego, C.; Shleev, S.; Fernandez, V. M.; De Lacey, A. L. *J. Phys. Chem. C* **2011**, *115*, 13420−13428.
(15) Blanford, C. F.; Foster, C. E.; Heath, R. S.; Armstrong, F. A. *Faraday Discuss.* **2008**, *140*, 319−335.
(16) Blanford, C. F.; Heath, R. S.; Armstrong, F. A. *Chem. Commun.* **2007**, 1710−1712.
(17) Sosna, M.; Chretien, J.-M.; Kilburn, J. D.; Bartlett, P. N. *Phys. Chem. Chem. Phys.* **2010**, *12*, 10018−10026.
(18) Thorum, M. S.; Anderson, C. A.; Hatch, J. J.; Campbell, A. S.; Marshall, N. M.; Zimmerman, S. C.; Lu, Y.; Gewirth, A. A. *J. Phys. Chem. Lett.* **2010**, *1*, 2251−2254.
(19) Szamocki, R.; Flexer, V.; Levin, L.; Forchiasin, F.; Calvo, E. J. *Electrochim. Acta* **2009**, *54*, 1970−1977.
(20) Scodeller, P.; Carballo, R.; Szamocki, R.; Levin, L.; Forchiassin, F.; Calvo, E. J. *J. Am. Chem. Soc.* **2010**, *132*, 11132−11140.
(21) Decher, G. *Science* **1997**, *277*, 1232−1237.
(22) Hodak, J.; Etchenique, R.; Calvo, E. J.; Singhal, K.; Bartlett, P. N. *Langmuir* **1997**, *13*, 2708−2716.
(23) Calvo, E. J.; Etchenique, R.; Pietrasanta, L.; Wolosiuk, A.; Danilowicz, C. *Anal. Chem.* **2001**, *73*, 1161−1168.
(24) Calvo, E. J.; Battaglini, F.; Danilowicz, C.; Wolosiuk, A.; Otero, M. *Faraday Discuss.* **2000**, *116*, 47−65.
(25) Calvo, E. J.; Flexer, V.; Tagliazucchi, M.; Scodeller, P. *Phys. Chem. Chem. Phys.* **2010**, *12*, 10033−10039.
(26) Laurent, D.; Schlenoff, J. B. *Langmuir* **1997**, *13*, 1552−1557.
(27) He, P. L.; Hu, N. F.; Rusling, J. F. *Langmuir* **2004**, *20*, 722−729.
(28) Caruso, F.; Niikura, K.; Furlong, D. N.; Okahata, Y. *Langmuir* **1997**, *13*, 3422−3426.
(29) Danilowicz, C.; Corton, E.; Battaglini, F. *J. Electroanal. Chem.* **1998**, *445*, 89−94.
(30) Shiratori, S. S.; Rubner, M. F. *Macromolecules* **2000**, *33*, 4213−4219.
(31) Folkesso, B. *Acta Chem. Scand.* **1973**, *27*, 287−302.
(32) Klein, J. C.; Proctor, A.; Hercules, D. M.; Black, J. F. *Anal. Chem.* **1983**, *55*, 2055−2059.